Beam Request

The separation of spin-singlet and triplet Λp amplitudes and final state interactions through the measurement of the spin correlation in the $\vec{p}\vec{p} \to K^+\Lambda p$ reaction at ANKE

S. Barsov, S. Mikirtytchiants[1], Yu. Valdau[1]
Petersburg Nuclear Physics Institute, 188350 Gatchina, Russia

D. Chiladze[2], R. Engels, R. Gebel, K. Grigoryev, M. Hartmann, A. Kacharava, B. Lorentz, D. Mchedlishvili[2], M. Mikirtytchiants, H. Ohm, D. Prasuhn, F. Rathmann, R. Schleichert, R. Stassen, H. Stockhorst, H. Ströher
Institut für Kernphysik, Forschungszentrum Jülich, 52425 Jülich, Germany

P. Goslawski, A. Khoukaz, M. Mielke, M. Papenbrock, D. Schröer
Institut für Kernphysik, Universität Münster, 48149 Münster, Germany

S. Dymov[3], E. Steffens
Physikalisches Institut II, Universität Erlangen–Nürnberg, 91058 Erlangen, Germany

T. Azarian, V. Komarov, A. Kulikov, V. Kurbatov, G. Macharashvili[2], S. Merzlyakov[1], V. Serdyuk[1], V. Shmakova[1], S. Trusov[1], D. Tsirkov, Yu. Uzikov
Joint Institute for Nuclear Research, 141980 Dubna, Russia

N. Lomidze, M. Nioradze, M. Tabidze
High Energy Physics Institute, Tbilisi State University, 0186 Tbilisi, Georgia

C. Wilkin
Physics and Astronomy Department, UCL, London WC1E 6BT, UK

Spokespersons: S. Barsov, Yu. Valdau and C. Wilkin
for the ANKE Collaboration

Jülich, January 13, 2014

[1] also in IKP, Forschungszentrum Jülich
[2] also in HEPI, Tbilisi
[3] also in JINR, Dubna

Abstract

The physics case of this proposal was accepted by the PAC session 41. The present document summarizes the first results of background studies, storage cell commissioning and the cell diameter optimisation.

The test beam time, taken in November 2013, has demonstrated the feasibility of C_{NN} studies using the magnetic spectrometer ANKE with polarised beam and target. The new ANKE openable and closable storage cell system has been commissioned and worked extremely reliably during the whole experiment. The target thickness obtained using the Schottky method was in a perfect agreement with the expectations for a 12 mm (diameter) storage cell. After analysis of the beam profiles, studied using the COSY Ionization Profile Monitor (IPM) and ANKE Silicone Tracking Telescope (STT), it is clear that a storage cell of 10 mm diameter is optimal for C_{NN} measurements at 1.662 GeV. A good signal of the Λ hyperon was identified for the first time from the experimental data obtained with a polarised gas target.

Summarizing, after a very successful commissioning beam time, we are ready to perform measurements of C_{NN} in the $\vec{p}\vec{p} \to K^+ p\Lambda$ reaction at $T_p =$ 1.662 GeV using ANKE. In order to reach the desired precision, **10 weeks** of beam time, accompanied by a sufficient number of machine development weeks, are needed.

1 Introduction

Following the recommendations of PAC41, a commissioning beam time took place in November 2013. This document summarises the results of the online analysis of the data accumulated during this beam time. More advanced analysis will be given in the presentation to PAC42.

2 COSY beam parameters

It has been shown several times that, with one week of machine development, it is possible to prepare a polarised proton beam ($\approx 75\%$) with a momentum up to 2.95 GeV/c with an intensity of the order of $\approx 5 \times 10^9$. To reach a high degree of polarisation together with a high beam intensity it is necessary to invest an additional week of machine development in order to optimise the beam intensity. This, together with plans to set up a Stochastic Cooling system, to cool the beam at the flat top energy, led us to decide to skip the beam polarisation question in the commissioning run. Hence, all the measurements during this beam time were done with an unpolarised proton beam.

2.1 Beam intensity and polarisation

The intensity of the unpolarised proton beam during the commissioning run was not very high, 5×10^9 protons/s at the flat top after acceleration per single injection. Using multiple injections (stacking), the intensity of the proton beam at the flat top has reached 2×10^{10} protons/s. It is expected that during the experiment with a polarised beam, after one week of machine development dedicated to the stacking optimisation, intensities of approximately $20 - 50\%$ of the unpolarised can be achieved, while preserving the high degree of polarisation. Therefore, for making beam-time estimates, we will assume 5×10^9 protons/s as the expected intensity of a polarised proton beam.

Since the commissioning run was carried out with an unpolarised proton beam, no beam polarisation measurements were made. It is planned to control the beam polarisation using the EDDA polarimeter at the end of each cycle of the experimental run. This method of beam polarimetry has already been used in several ANKE experiments and allows one to evaluate the beam polarisation with a statistical precision of better then 1 % and overal systematic precision of $\approx 5\%$ for every pair of cycles [1]. For the beam-time estimates, we assume a polarisation of 60%.

2.2 Beam emittance

The emittance of the proton beam depends primarily on the beam energy, the number of particles, and the heating and cooling forces available in the ring. It is extremely important for this experiment to keep the beam emittance as small as possible, not only at injection but also throughout the whole cycle of measurements.

Heating forces in the accelerator are intimately connected with the overall vacuum conditions in the ring. During the experiment in November 2013 the vacuum conditions in all sections of COSY were relatively good. The individual pressure in all the sections of the storage ring, except ANKE, was kept below $\approx 10^{-8}$ torr (see Fig. 1).

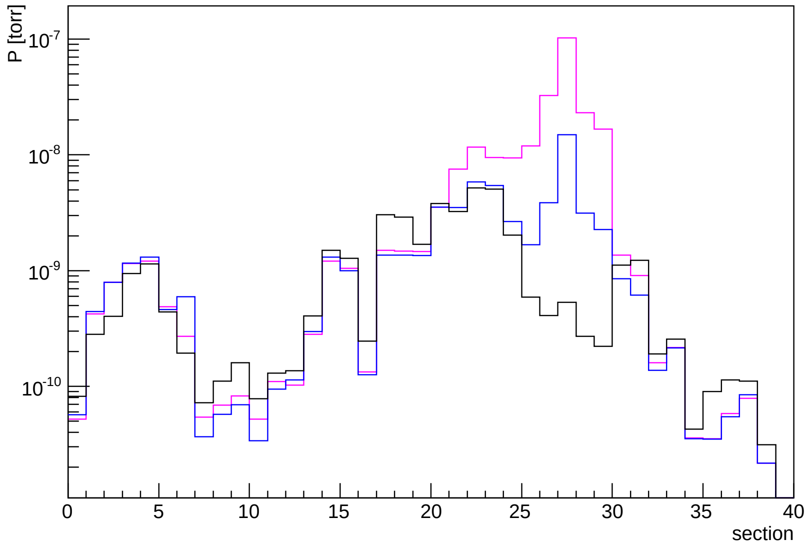

Figure 1: Vacuum conditions before (black line) the installation of the ANKE storage cell, with the storage cell in the target chamber (blue line), and during normal operation of the storage cell, with polarised hydrogen from the ABS (magenta line), and the Silicone Tracking Telescope (STT).

Figure 1 compares the vacuum conditions in the COSY ring before the installation of the storage cell and with the storage cell and polarised hydrogen gas from the ABS. It is clear that the vacuum conditions in the ANKE region (sections 25-31) are significantly influenced, not only by additional equipment in the target chamber, but also by a polarised internal gas target. The vacuum conditions in other sections of the accelerator can be and are improved with time by using Titanium sublimation pumps, as one can see from Fig. 1. However, due to the relatively low beta function in the ANKE target chamber region, the vacuum conditions there do not influence the beam size very significantly.

At the energy of the experiment ($T_p = 1.662$ GeV), only a Stochastic Cooling (SC) system is available at COSY, but the beam can be pre-cooled at injection energy by using a 100 keV electron cooler. The new 2 MeV e-cooler, although already in a commissioning phase, is not yet ready to provide cooling at the energy of the experiment. Furthermore, in the construction of the 2 MeV e-cooler no compensation coils were foreseen for the cooler solenoid. Therefore, experiments with this cooler and polarised beams will require solenoidal field compensation in some other place in the ring, for example, by using a Siberian snake. But all these techniques have still to be developed.

During the machine development, the beam emittance has been studied by using the Ionisation Profile Monitor of COSY (IPM). Figure 2 presents the beam profiles measured under different beam conditions as a function of time at the energy of the experiment.

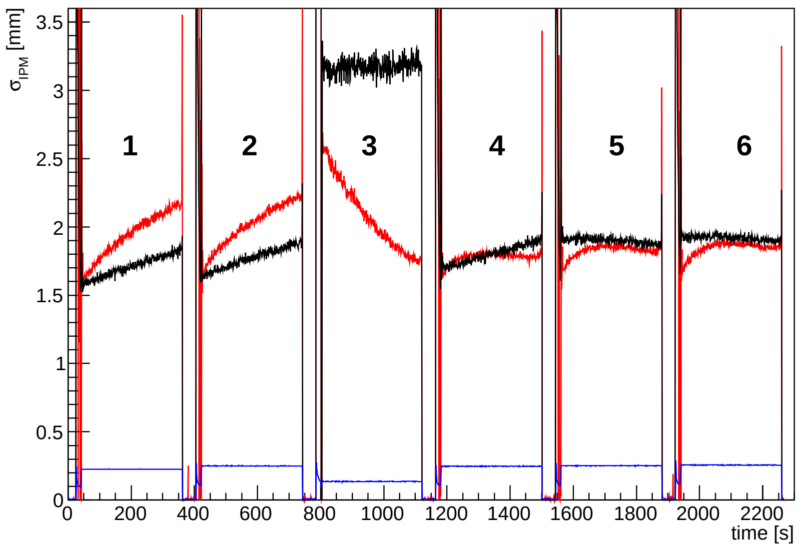

Figure 2: Beam size (σ) in the horizontal (red) and vertical (black) directions and beam current (blue line, arbitrary units) measured with the COSY-IPM under different beam conditions before installation of the ANKE storage cell. Cycle 1 - only electron cooling at injection energy is working. Cycle 2 - The Barrier-Bucket system is on. Cycle 3 - The Barrier-Bucket system is on, e-cooler at injection energy is off, Stochastic Cooling in the X plane. Cycle 4 - Barrier-Bucket system is on, e-cooler at injection energy is on, Stochastic Cooling in the X plane. Cycle 5 - Barrier-Bucket system is on, e-cooler at injection energy is on, Stochastic Cooling in the X and Y planes. Cycle 6 - Barrier-Bucket system is on, e-cooler at injection energy is on, Stochastic Cooling in the X and Y planes, ANKE ABS jet in the target chamber.

From the data shown in Fig. 2, it is clear that the beam size in the region of the IPM at the energy of the experiment is about ≈ 2 mm. The measurements were done at the flat top with almost constant beam intensity of 9×10^9 protons/s. The comparison of the first and second cycles in Fig 2 shows that the Barrier-Bucket system does not influence the beam size at the energy of the experiment but can be used to compensate for the mean energy loss during the experiment. By comparing the third and fourth cycles it is seen that the pre-cooling procedure at the injection energy is very effective and defines the beam size at the energy of experiment. The Stochastic Cooling system in the X and Y planes are operational and can cool effectively the beam to the equilibrium size, which is also about 2 mm in both directions (see cycles 4, 5, and 6). From the results obtained during cycle 6, it is clear from Fig. 2 that the jet from the ANKE ABS will not give enough heating of the beam to disturb the beam size.

Unfortunately, the COSY stochastic cooling system has not been used for several years and it was therefore difficult to bring it back into operation during the time available for machine development. Due to the unstable behaviour of the individual components of the Stochastic Cooling system for the X plane, it was only demonstrated that cooling of the proton beam at a momentum of 2.425 GeV/c is possible, but most of the data were collected without its use.

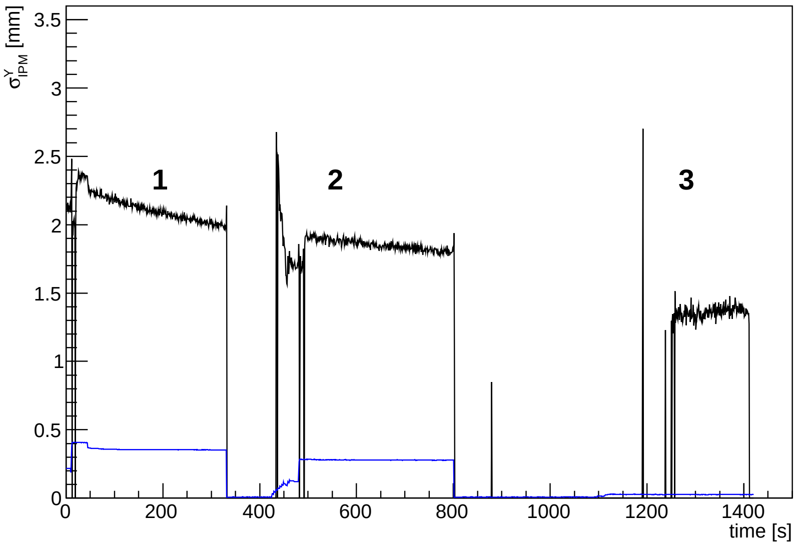

Figure 3: Vertical beam size (σ) and beam current (blue line, arbitrary units) measured with the COSY-IPM after installation of the ANKE storage cell and STT. The data were collected in identical beam conditions, but with the number of particles at the flat top being 1.4×10^{10}, 1.0×10^{10} and 4×10^{8} protons/s for the first, second and third cycle, respectively. The IPM was not operational during part of the third cycle.

The influence of number of particles at the flat top on the vertical beam size has been studied in Fig. 3. The measurements were done after all the ANKE systems had been installed in the ANKE target chamber and with polarised hydrogen gas in the storage cell. This means that the vacuum conditions in the ANKE region were significantly different from those in which the beam profiles of Fig. 2 were obtained. The e-cooler at injection and Stochastic Cooling in vertical direction were in operation all the time. A change in beam intensity of 30% changes the vertical beam size by 13% so that the influence of the number of particles in the beam on σ_Y is relatively weak. Measurements with very low beam intensity show (cycle 3 in Fig. 3) that the beam size at the experimental energy is limited by other effects. We therefore conclude that up to 2×10^{10} polarised protons can be stacked into COSY without significant change of beam size and hence not limiting storage cell diameter.

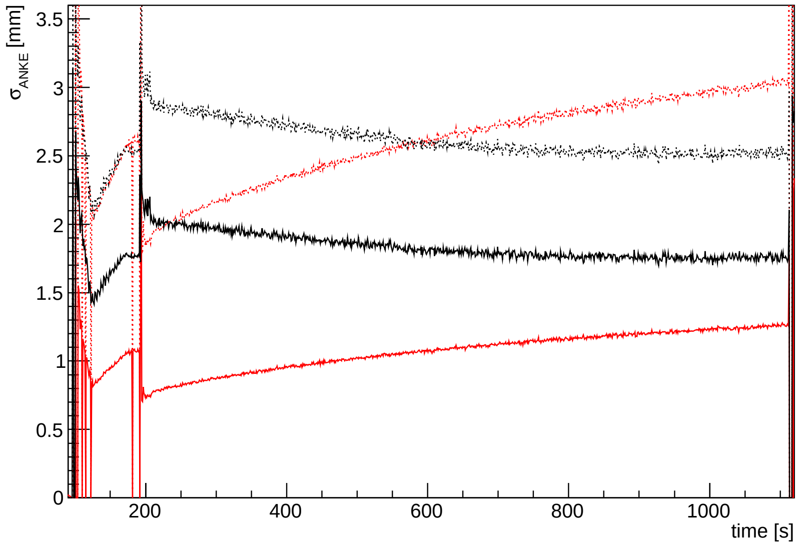

Figure 4: Vertical (black) and horizontal (red) beam size as a function of time in a cycle measured with the IPM (dotted line) and recalculated to the ANKE target position (solid line). The measurements were done with 1.8×10^{10} protons in the ring, with pre-cooling using the e-cooler at injection energy and stochastic cooling system in the Y direction. The closed ANKE storage cell was filled with polarised hydrogen gas from the ABS.

2.3 Beam size at the ANKE target position

Using the data measured with the IPM it is possible to estimate the beam size at the ANKE target position in terms of the difference in the beta functions and dispersions at these two points in the ring. The values of the beam size in the horizontal and vertical directions thus obtained at the ANKE target place are presented in Fig. 4. The measurements were done in the conditions that were later used during the whole experiment: stacking at injection, pre-cooling using the e-cooler, stochastic cooling only in the Y plane, ANKE storage cell closed and filled with polarised gas from the ABS. The beam intensity at the flat top was approximately 1.8×10^{10} protons/s.

The vertical beam size in the ANKE target chamber, as obtained from the IPM measurements, are in reasonable agreement with the values extracted from *pd* scattering measured using the ANKE Silicone Tracking Telescope (STT) installed close to the storage cell (see Fig. 5).

Studies performed during this commissioning run have demonstrated that the COSY beam size in the ANKE target chamber at the energy of the experiment is below $\sigma \approx 2$ mm in the vertical and horizontal directions and that this can be kept around this value over all the measurement cycle by using the COSY Stochastic Cooling system. Hence for the real experiment it is possible to use a storage cell with tube diameter of 10 mm, if this can be produced using the technologies available in the ZEA of the Forschungszentrum Jülich.

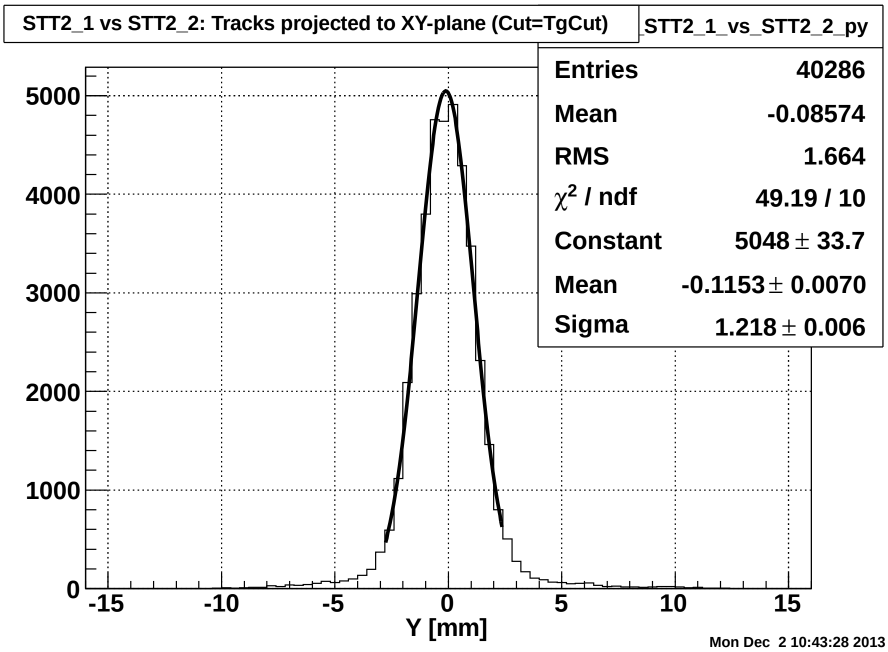

Figure 5: The vertical beam size measured using a Fd and STT coincidence in ANKE. The $\sigma_Y = 1.2$ mm value obtained from the ANKE analysis is in reasonable agreement with the IPM measurements presented in Fig. 4.

3 Commissioning of the ANKE polarised internal gas target

In this section the results of the commissioning of the ANKE polarised internal gas target are summarised. Due to the common effort of the ANKE collaboration in the preparation for the double-polarised experiments #213 and #219, the contents of Secs. 3.1 and 4 are identical in the two proposals presented to PAC41.

3.1 ANKE openable/closable storage cell

One of the main goals in the commissioning run was to bring a new openable/closable storage cell into operation. The ANKE storage cell was built in the ZEA of the Forschungszentrum Jülich. As illustrated in Fig. 6, it is made up of two tubes welded to the rectangular block of material with an opening/closing mechanism. The long tube (storage tube), which is welded to the rigid block of material with a hall, is cut into two halves along its length. The second tube (injection tube) is connected to the same metallic block of material inside which the injection and storage volume are connected. The storage cell is 390 mm long and has an inner diameter 11.8 mm. The feeding tube is 130 mm long and has an inner diameter of 11.8 mm. Each half of the storage cell can be moved up and down using precision piezoelectric drives. Each individual drive provides a precision in positioning of the order of < 1 μm [2]. All cell parts are covered by a 30 μm PTFE [3] coating designed to minimize recombination effects. [4].

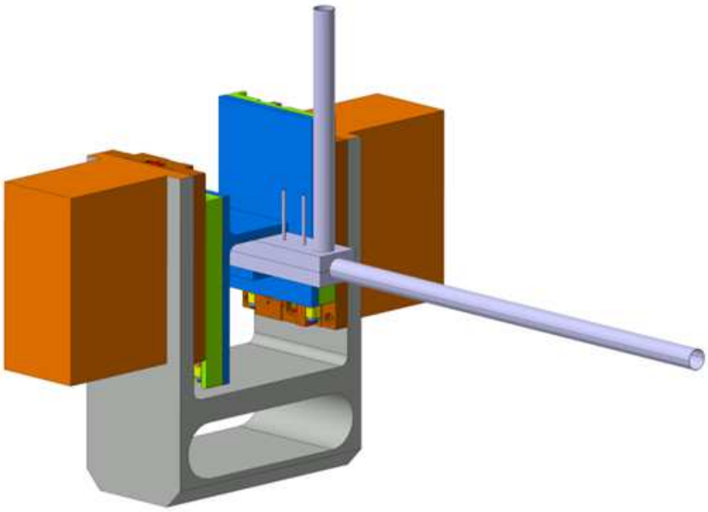

Figure 6: The principle of the ANKE cell construction. It consist of two tubes, one injection tube to introduce the ABS gas and the storage tube that keeps the polarised gas in the interaction region. Both tubes are welded to the rigid metallic block to preserve the coplanarity in the system. The storage tube and block are cut into two halves along the long side. The halves can be moved up and down using piezoelectric motors (green parts) which are connected using special support (blue parts) to the each half of the block. The yellow parts in the picture are protection for the STTs which, in the final version, can be parked behind them during injection.

During the machining and cutting of the storage cells, special attention was paid to retaining the coplanarity of the halves. If there were a gap between the two halves of the cell of the order of 50 μm then a significant fraction of the target thickness (up to 20%) in the beam-target interaction region could be lost. The stainless steel storage cell, used during commissioning run, was very tight and no visible gap between two halves was observed before and after the beam time.

The expected target thickness distribution has been calculated as a function of the coordinate for the storage cell of this dimension and later measured in the laboratory using Baratron [5] and none-cut cell. The results of the measurements are compared to the calculations in Fig. 7, where it is seen that the agreement is very good. The integrated target thicknesses from the calculations and measurements in the laboratory are in a good agreement.

The first storage cell shown in Fig. 8 had an inner diameter of 11.8 mm and was produced from stainless steel (wall thickness 100 μm) covered with Teflon. During the test run with this stainless steel cell the target thickness was measured at different energies using the Schottky method [6]. Thicknesses of about 3×10^{13} were

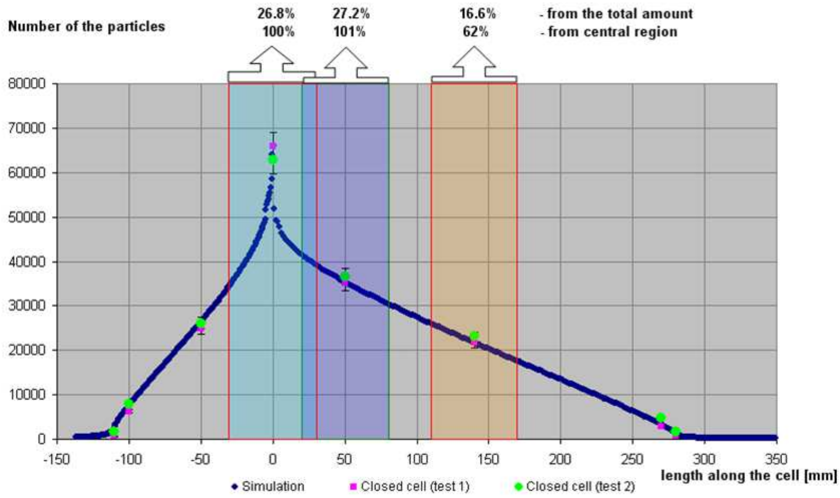

Figure 7: Target thickness in the storage cell as a function of coordinate along the beam direction. The calculations (blue symbols) are compared to the measurements (magenta and green symbols) for the 12 mm storage cell.

obtained for hydrogen and deuterium. The measured value of the target thickness for the hydrogen is in good agreement with the expected thickness.

Figure 8: Photograph of the opened ANKE storage cell mounted on a flange in the laboratory. Also shown are the Piezoelectric drivers for opening/closing the tube, the STT installation, the plastic tubes for the Baratron to control the pressure, and the unpolarised gas supply system (UGSS).

Since the target polarisation with the stainless steel cell was low, a second cell prototype was built from Titanium (inner diameter 11.6 mm, wall thickness 200 μm, feeding tube inner diameter 10 mm) and covered with 30 μm PTFE. Due to mechanical imperfections, the target thickness for the Titanium cell was lower then for the stainless steel cell. Using the Schottky method a value of $\approx 1.8 \times 10^{13}$ cm^{-2} for hydrogen target was found.

4 Target polarisation with the openable storage cell

The first approach to the cell construction was through the use of stainless steel for the walls. This type of cell was tested in the November 2013 beam time and the results of these tests are presented in Sections 4.1–4.3. The low value of the polarisation achieved in the steel cell required a change in the construction material. A new cell with titanium walls was tested with the COSY beam in mid-January 2014 and the excellent results obtained are described in Section 4.4.

The target polarisation was studied with nuclear reactions that were accessible under the conditions of the two experiments being commissioned (proposals #213 and #219). Both pp elastic scattering and the $pp \to d\pi^+$ reaction were used for this purpose with the hydrogen gas target. The polarisation of the $\vec{\mathrm{D}}$ target was defined with the use of $pd \to pd$ elastic scattering and the quasi-free $pp \to d\pi^+$ reaction. The necessary analysing powers in these reactions are available from the literature.

Elastic scattering reactions were recorded with the STT, which covered only about a 5 cm long region of the cell (the cell length is 39 cm). The (quasi)-free $pp \to d\pi^+$ process, with both final particles detected in the ANKE forward (Fd) or Positive (Pd) detectors, allowed estimates to be made of the average gas polarisation over the whole cell, as well as the study of the distribution of the polarisation along the cell. Neither the $T_p = 1.66$ nor 0.353 GeV beam energy is suitable for a polarimetry study on the basis of the $pp \to d\pi^+$ process, for which the optimal is ≈ 580 MeV. Thus, dedicated runs were undertaken at this energy with both $\vec{\mathrm{H}}$ and $\vec{\mathrm{D}}$ targets.

To save time and effort during the commissioning, both experiments were conducted with the same ANKE D2 magnet deflection angle of $\alpha = 8.44^\circ$, which is optimal for the experiment at 1.66 GeV. For the 353 MeV experiment, this meant the use of the 0.55 Tl magnetic field of the ANKE D2 magnet, instead of the 0.70 Tl foreseen for the main experiment at $\alpha = 10.6^\circ$. However, the field value at 580 MeV and 8.44° is 0.75 Tl, so that the polarimetry results obtained at this energy fit the commissioning goals of the experiment at 353 MeV.

To accomplish the polarisation study with the cell, one had to ensure a high value of polarisation of the gas in the ABS jet. The measurements with the Lamb Shift polarimeter could not provide the absolute values of the polarisation. Thus, a separate measurement of the jet polarisation with nuclear reactions was done, with the cell removed from the target chamber.

We present below the results of this series of measurements.

4.1 Polarimetry with the steel cell at 580 MeV

This measurement was performed early in the beam time, before the STT had been installed. Thus, the only polarimetry reaction employed was the (quasi)-free $pp \to d\pi^+$. The ejectile deuteron from this process was detected in the Fd, while the pion hit either the Fd or Pd. The $d\pi^+$ pairs were clearly identified through the time-of-flight (TOF) difference of the two particles and the process was then selected

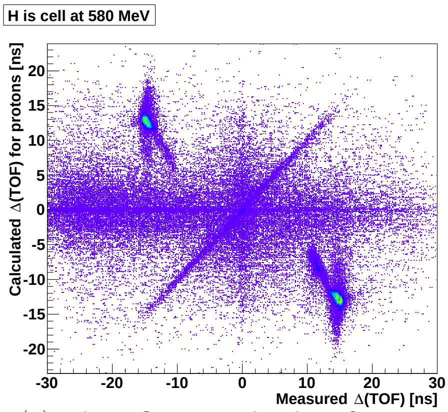

(a) The TOF particle identification

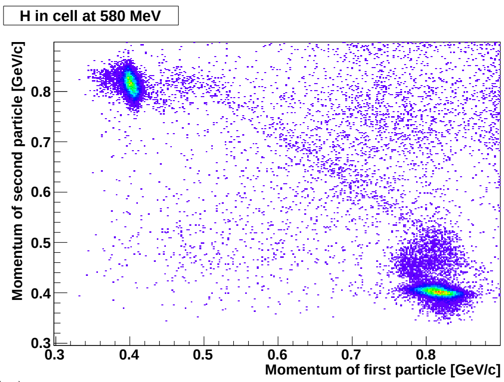

(b) Momentum correlation of two tracks in the Forward detector

Figure 9: $pp \to d\pi^+$ reaction identification at 580 MeV

kinematically. In Fig. 9(a) the measured TOF difference of the two particles is compared to the one estimated under the assumption that the two charged particles each have the proton mass. The $d\pi^+$ pairs are located in the two bright spots in the figure. The correlation of the momenta of the two particles detected in Fd is

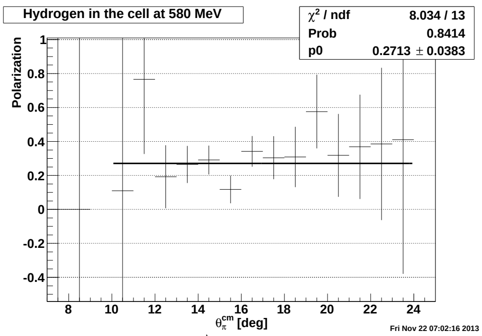

(a) $\vec{\mathrm{H}}$ in the cell

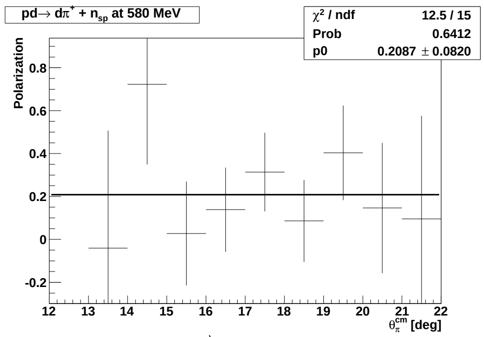

(b) $\vec{\mathrm{D}}$ in the cell

Figure 10: Target polarisations measured with the stainless steel cell at 580 MeV

shown in Fig. 9(b), where the $pp \to d\pi^+$ events also group into two regions at $\sim (0.4, 0.8)$ GeV/c. The analysing power in this process is available from the SAID data base [10] and reaches 0.2 in the angular range of our experiment, $\theta_\pi^{cm} = (12 - 24)^\circ$. The results of polarisation determination with $\vec{\mathrm{H}}$ and $\vec{\mathrm{D}}$ targets are shown in Fig. 10. The values of $Q(\vec{\mathrm{H}}) = 27 \pm 4\%$ and $Q(\vec{\mathrm{D}}) = 21 \pm 8\%$ are close to those obtained with a cell of stainless steel [4].

The measurement of the time-of-flight difference allows the possibility to reconstruct the longitudinal coordinate Z of the reaction vertex. In the case of the hydrogen target, the kinematical constraints improve the accuracy of this coordinate down to $\sigma_Z = 5$ cm (Fig. 11(a)), so that one can study the distribution of the polarisation along the cell, as shown in Fig. 11(b). One can see that, within our limited statistics, no substantial change of the polarisation is observed within the cell $Z = (-136, -97)$ cm, with a possible reduction in the region outside of the cell.

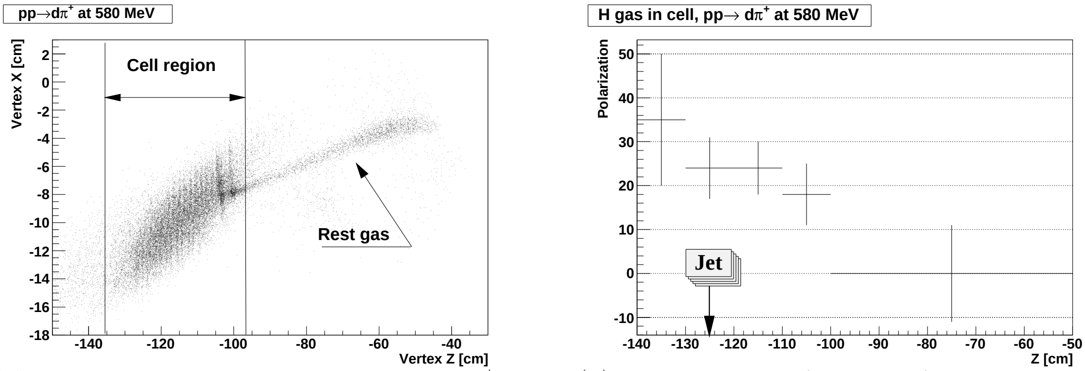

(a) Vertex reconstructed for $pp \rightarrow d\pi^+$ events

(b) Polarisation as function of the longitudinal coordinate

Figure 11: Measurement with $\vec{\mathrm{H}}$ with the stainless steel cell at 580 MeV

4.2 Polarimetry with the steel cell at 1.66 GeV

Both the cross section and analysing power of the $pp \rightarrow d\pi^+$ reaction in the angular range of the ANKE acceptance are too low at this energy and the polarisation could only be measured reliably with pp elastic scattering. The two final protons from the latter were recorded in coincidence in the Fd and STT. The recoil proton in STT could be identified through the energy loss and the process was selected by the kinematics.

The pp elastic scattering analysing power was measured during the ANKE beam time in March 2013 [11] at 1.6 GeV in the angular range of interest of $\theta_p^{cm} = (15-25)^\circ$, and only a small change of 4% is expected for A_y between the 1.6 and 1.66 GeV beam energies.

A polarisation of $19 \pm 3\%$ was obtained, which is consistent with the results at 580 MeV. At this beam energy only the $\vec{\mathrm{H}}$ target polarisation is of interest.

4.3 Polarimetry with the ABS jet

A special feature of this measurement is the low target density in the jet, amounting to $\sim 10^{11}\mathrm{at/cm}^2$. One consequence of this was that the count rate was too low for the $pp \rightarrow d\pi^+$ reaction even at 580 MeV to collect reasonable statistics within the time available. Furthermore, the jet density was comparable to that of the rest gas in the vacuum chamber. It was therefore necessary to select the jet region directly, using the tracks reconstructed in STT. With this aim in mind, after the cell removal, the STT was moved to a position close to the jet and the polarisation of the $\vec{\mathrm{H}}$ and $\vec{\mathrm{D}}$ jets was defined by pp and pd elastic scattering, respectively.

The measurement at 1.66 GeV with the $\vec{\mathrm{H}}$ jet was done in a similar way to the cell. It resulted in a jet polarisation of $59 \pm 2\%$. Although significantly higher than that found with the cell, this value is lower than that expected from the laboratory ABS tests (91%). The reasons for this reduction have still to be discovered.

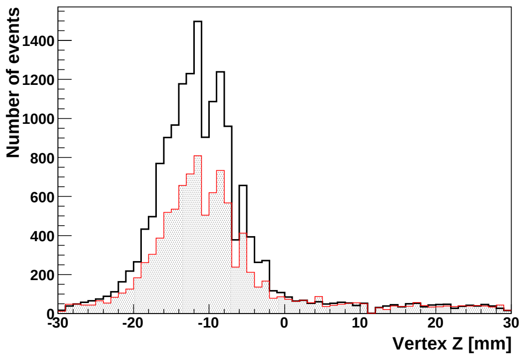

Figure 12: Vertex Z coordinate reconstructed from the STT measurements with ABS jet at 580 MeV. The counts for ABS polarisation-up are shown by the thick line, and for polarisation-down by the filled histogram.

At 580 MeV, the polarisations of both the $\vec{\mathrm{H}}$ and $\vec{\mathrm{D}}$ jets have been measured. The pp elastic scattering analysing power is well described at this energy by the SAID phase shift analysis. Figure 12 shows the distribution of the longitudinal vertex coordinate Z reconstructed from the STT data. One can clearly see the jet peak surrounded by the unpolarised rest gas background. In the other measurements with the jet the distributions were very similar. The measured polarisation of the jet was $85 \pm 4\%$.

The analysing powers in $pd \to pd$ elastic scattering were measured at energies close to 580 MeV at Argonne and ANKE [12, 13]. Although the nominal tensor polarisation of the $\vec{\mathrm{D}}$ jet for the modes chosen was equal to 1, it introduced only a $\sim$ 10% correction to the estimated vector polarisation of the jet. In this measurement, the recoil deuteron was stopped in the second layer of he STT and thus could be clearly identified by its energy loss. The resulting deuterium polarisation was $80 \pm 5\%$.

4.4 Measurement with the titanium cell

The measurement was conducted for both $\vec{\mathrm{H}}$ and $\vec{\mathrm{D}}$ targets with the 580 MeV proton beam, using the $pp \to d\pi^+$ reaction for the polarimetry in the same way as described in section 4.1. The results obtained with the hydrogen target are shown separately in Fig. 13 for events originating in the cell region (a) and for the rest gas in the target chamber (b). The value of the polarisation in the cell is $Q = 86 \pm 5\%$, which is only 5% lower than the highest jet polarisation observed in the laboratory tests. As expected, the rest-gas polarisation is very low, which supports the correctness of the analysis.

The polarisation of the deuterium target was $61 \pm 10\%$. This value is consistent with the one obtained from the deuterium target commissioning run in 2012 $Q =$

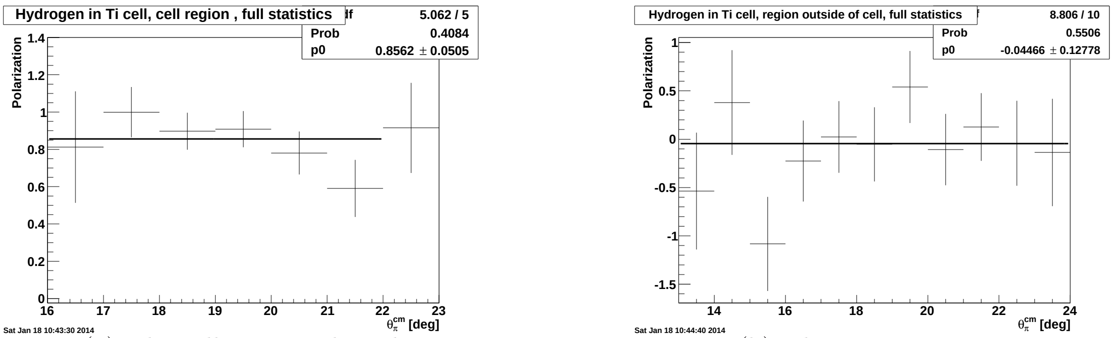

(a) The cell region selected (b) The rest-gas region

Figure 13: $\vec{\mathrm{H}}$ target polarisations measured with the titanium cell at 580 MeV

$72 \pm 1\%$ [14]. Based on the small polarisation loss observed with the hydrogen target, one can reasonably assume a polarisation value of 70% for the count rate estimations.

5 General statistical considerations for C_{NN}

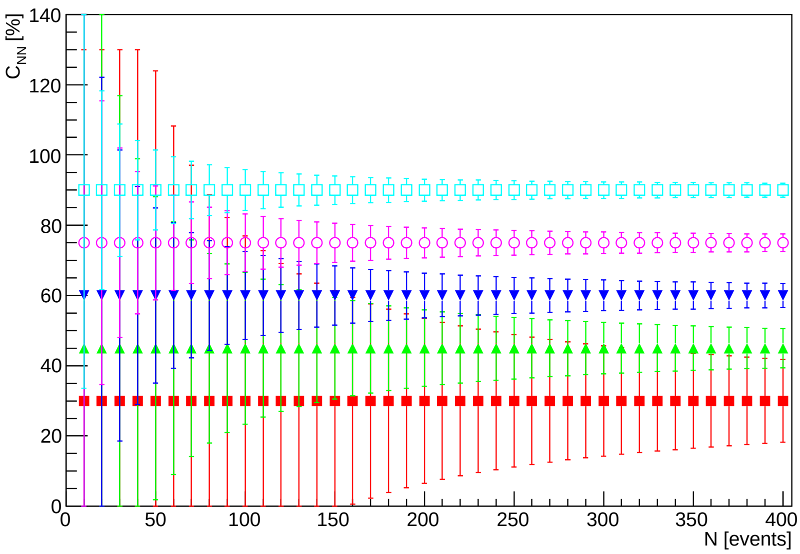

Figure 14: Predicted values of C_{NN} for the $\vec{p}\vec{p} \to K^+\Lambda p$ reaction, together with expected statistical errors, as a function of the number of events in each individual bin. Calculations are done for C_{NN} values of 0.3 (red), 0.45 (green), 0.6 (blue), 0.75(magenta) and 0.9(light blue) assuming beam and target polarisation of $60\pm1\%$. The error bars are statistical.

The C_{NN} can be written:

$$C_{NN} = \frac{1}{P \times Q} \frac{N_1 - N_2}{N_1 + N_2}. \tag{5.1}$$

where P and Q are the beam and target polarisations, while the N_1 and N_2 number of events with parallel and antiparallel directions of beam and target polarisations.

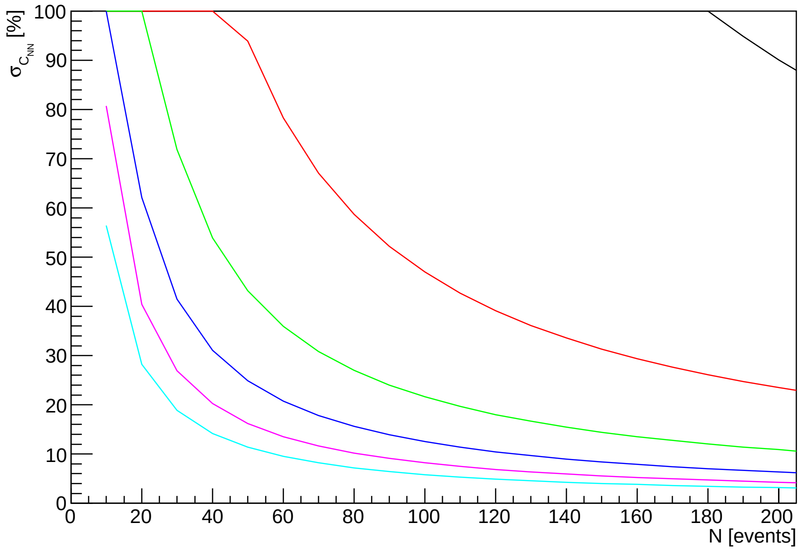

Figure 15: Expected statistical error in C_{NN} as a function of the number of detected events in an individual bin, calculated for the beam and target polarisation of $60 \pm 1\%$. Calculations for C_{NN} values of 0.15, 0.3, 0.45, 0.6, 0.75 and 0.9, are presented by black, red, green, blue, magenta, and light blue lines, respectively.

Figure 14 shows C_{NN} as a function of the number of events in bin together with its statistical error on the assumption that the beam and target polarisations are equal to 60% with a statistical precision of 1%. From the present simplified calculations it is clear that, in order to determine a C_{NN} below 30%, it is necessary to accumulate more than 400 events in a bin. On the other hand, if C_{NN} is bigger than 45% then this number of events would give a statistical precision of $\sim 15\%$.

Figure 15 shows the statistical error in $\sigma_{C_{NN}}$ as a function of the number of events in a bin for different values of C_{NN}, assuming $60 \pm 1\%$ polarisation of beam and target. It is clear that, if C_{NN} is bigger than 45%, approximately 100 events per bin is sufficient to measure it to a precision of 20%.

In Fig. 16 the dependence of the statistical error $\sigma_{C_{NN}}$ for one bin with one hundred events is presented as a function of the polarisation of beam and target (for simplicity assumed equal) calculated for different fixed C_{NN} values. It is clear from this that, if the overall beam and target polarisations are below 60%, it is necessary to accumulate far more than a hundred events per bin in order to determine C_{NN} with a precision better than 50%.

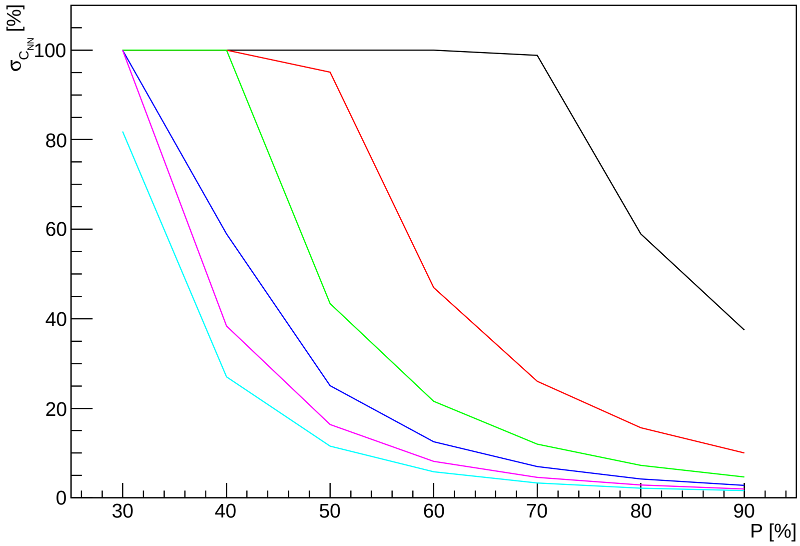

Figure 16: The statistical error $\sigma_{C_{NN}}$ as a function of the overall beam and target polarisations estimated for an individual bin with one hundred events. The calculations for C_{NN} values of 0.15, 0.3, 0.45, 0.6, 0.75, and 0.9 are presented by black, red, green, blue, magenta, and light blue lines, respectively.

6 Identification of the $pp \to K^+p\Lambda$ reaction with the storage cell

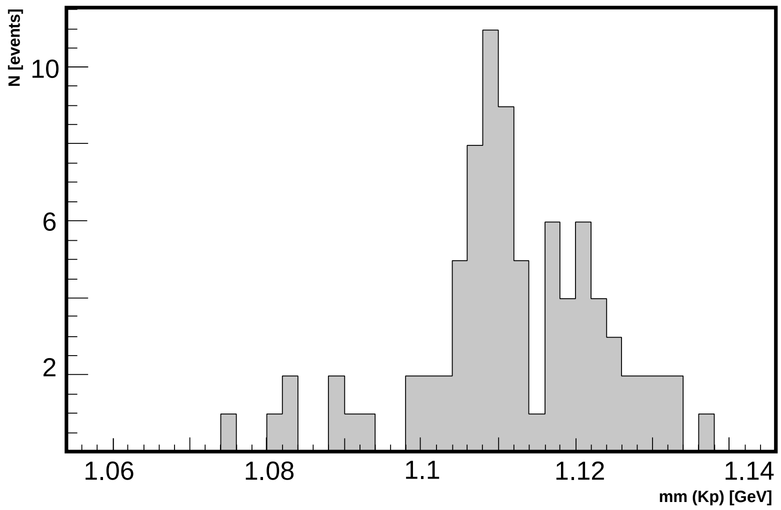

Figure 17: The K^+p missing-mass spectrum measured at 2.425 GeV/c during the commissioning beam time using the ANKE magnetic spectrometer with polarised internal gas target. The K^+p pairs are reconstructed using the delayed-veto technique. A signal from the Λ hyperon is clearly seen on top of a moderate background.

The K^+p missing-mass spectrum measured using the ANKE magnetic spectrometer and polarised internal gas target during the commissioning beam time is presented in Fig. 17. The spectrum is reconstructed from part of the statistics using a delayed-veto technique. A clean peak from the K^+p pairs associated with Λ hyperon production is seen in the distribution. The statistics obtained are in good agreement with the simulations done for the original proposal #219 [7] and presented during PAC 41.

The delayed-veto technique used to obtain the clean identification of the Λ hyperon (Fig. 17) has an efficiency of only $< 30\%$ [8], which means that the statistics obtained in this case are reduced by a factor of three. More careful analysis of the experimental data obtained during the commissioning beam time is needed in order to reconstruct the K^+p missing-mass spectrum without the use of the delayed veto. The results of this analysis will be presented during the open session of the PAC.

7 Experimental requirements

In Sec. 9 beam-time estimates are presented based on following values for the beam and target parameters:

- Polarised proton beam intensity of 5×10^9 protons. During the commissioning run, an unpolarised proton beam intensity with stacking was 2×10^{10} protons. With a polarised beam, after the same number of stacking, it is possible to reach 25% of unpolarised intensity.

- Polarisation of the proton beam 60%. Although, it was shown several times that it is possible to reach up to 75% polarisation of the beam, none of the recent ANKE experiments had a value higher than 55% [1].

- Target thickness of 6×10^{13} cm^{-2}. It should be possible to produce a 10 mm diameter storage cell from Titanium with a wall thickness of 100 μm.

- Target polarisation of 60%. As was shown in Sec. 4, Titanium is a good material to preserve the polarisation of a polarised gas in a storage cell. But, since the experiment has to be done with the highest D2 magnetic field, some inefficiency is possible, due to the none perfect shielding of the ABS transition units. The results of the ABS jet polarisation measurements at 2.425 GeV/c are presented in Sec. 4.

8 Simulations of the $pp \to K^+p\Lambda$ reaction

The estimations presented in this section are done on the basis of the parameters listed in Sec. 7. Simulations for the K^+p missing-mass spectrum, measured over ten weeks of beam time at ANKE using a polarised internal gas target, are presented in Fig. 18. The Λ peak is well identified on the top of the smooth physics background from the $\Lambda \to p\pi^-$ decay (BR 64%).

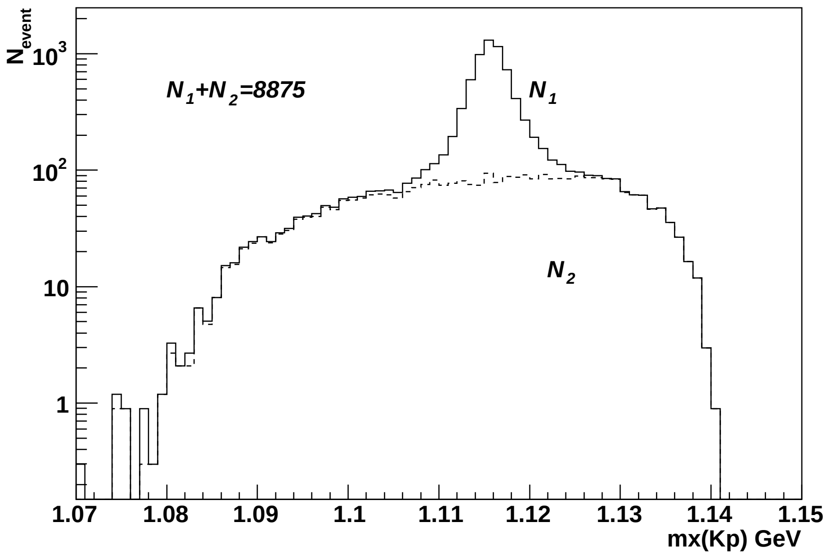

Figure 18: Simulation of the expected K^+p missing-mass spectrum for the $pp \to K^+p\Lambda$ reaction for the sum of all polarisation states after 10 weeks of beam-time measurements at ANKE. The peak in the distribution corresponds to the direct proton (N_1) from the $pp \to K^+p\Lambda$ reaction, while the smooth distribution underneath corresponds to K^+p pairs (N_2) where the proton originates from the $\Lambda \to p\pi^-$ decay.

Since it is planned to identify K^+p correlations using time-of-flight information, it is only possible to use direct protons (N_1) for the C_{NN} determination. Hence not all statistics in Fig. 18 can be used for the final analysis.

The ANKE acceptance is relatively symmetric as a function of the azimuthal angle ϕ, but this is not the case for the polar angle θ. In Fig. 19 simulation for the K^+ angular spectra measured after ten weeks of beam time for the sum of all states is presented. Although ANKE has acceptance in all the angular range there is a large forward-backward asymmetry, with very moderate statistics around $\cos\theta \approx 0$.

At the moment we have no reliable model for C_{NN} but, on the basis of simulations presented in Fig. 19 and using the formalism from Sec. 5, one can estimate possible statistical errors in individual bins of the angular spectra for different values of C_{NN}. The estimated errors in C_{NN} as a function of angle are presented in Fig. 20. The statistics expected after ten weeks are not very large and hence, if C_{NN} is below 30% in some of the bins, the statistical error will be relatively high. However, in the forward and backward regions, where the ANKE acceptance is high, even small C_{NN} can be determined with good precision in such a beam time.

Figure 21 presents the phase-space simulation of the K^+ missing mass for the $pp \to K^+p\Lambda$ reaction after ten weeks of measurements with ANKE. When C_{NN} is studied as a function of the missing mass, the statistics obtained have to be divided between the two polarisation states. On the basis of the calculations presented in Sec. 5, it is clear that, if there is a missing-mass dependence of C_{NN}, it is possible to determine it.

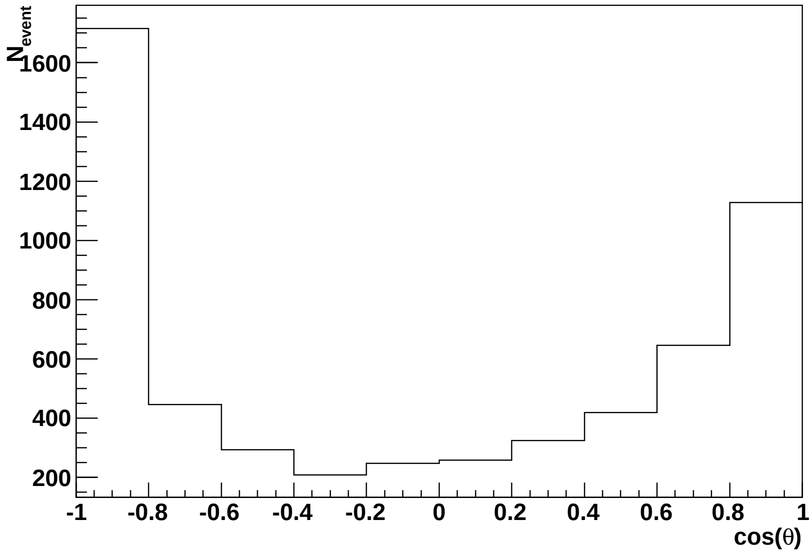

Figure 19: Simulation of the K^+ angular spectra from the $pp \to K^+p\Lambda$ reaction for the sum over all polarisation states after 10 weeks of measurements with the magnetic spectrometer ANKE. Only K^+p pairs with direct proton (N_1) are used in the distribution.

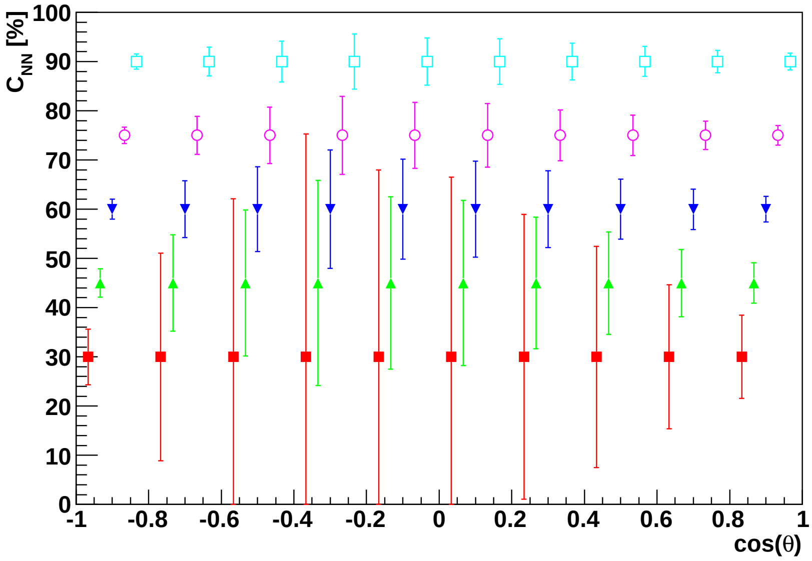

Figure 20: Simulations for the possible error in the determination of C_{NN} as a function of the K^+ angle after ten weeks of measurements at ANKE. Estimates were made for C_{NN} having values of 0.9 (red), 0.75 (light blue), 0.6 (magenta), 0.45 (blue), and 0.3 (red). For presentational reasons, symbols for different values of C_{NN} are shifted with respect to each other inside one $\cos\theta$ bin.

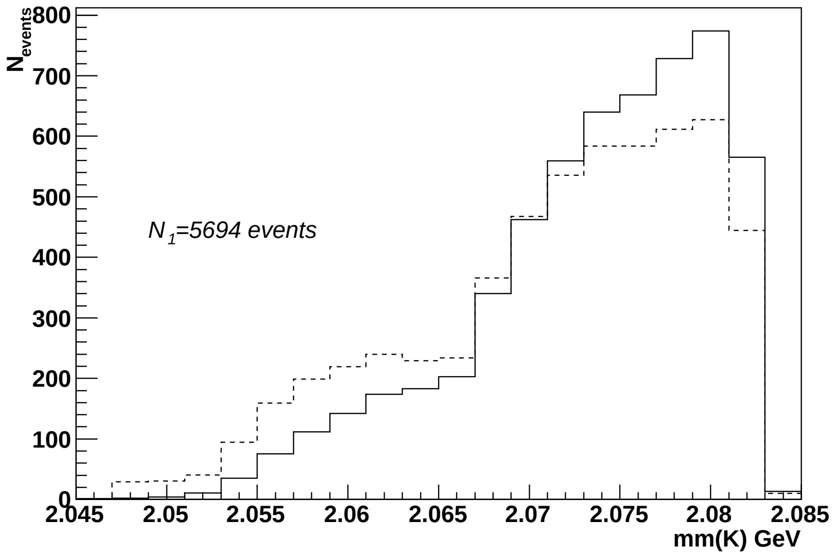

Figure 21: Phase-space simulations of the K^+ missing-mass spectra for the sum of all polarisation states after ten weeks of measurements at ANKE. The dashed line represents phase space modified the Λp final state interaction, with parameters taken from Ref. [9].

9 Beam Request

The proposed studies of C_{NN} for the $pp \to K^+ p\Lambda$ will yield following results:

- Fix the relative strengths of the singlet and triplet productions for the $pp \to K^+ p\Lambda$ reaction close to threshold.
- Measuring C_{NN} as a function of the K^+ momentum will give information on the relative strengths of the singlet and triplet $p\Lambda$ FSI, on which there is little direct information.

The total beam time needed to perform such an experiment at ANKE is **ten weeks** which should be accompanied by a sufficient number of machine development.

References

[1] Highlights section of the IKP Annual Report 2013.

[2] RS private communication.

[3] RS private communication.

[4] J.S. Price and W. Haeberli, NIMA **349** (1994) 321.

[5] MKS Baratron Type 690A, produced by MKS Instruments, Inc.

[6] H. J. Stein *et al.*, Phys. Rev. ST Accel. Beams **11** (2008) 052801.

[7] S. Barsov, A. Kacharava, C. Wilkin, COSY proposal #**219** (2013).

[8] M. Büscher *et al.*, Nucl. Instrum. Methods A **481**, 378 (2002).

[9] A. Budzanowski *et al.*, Phys. Lett. B **687** (2010) 31.

[10] R. A. Arndt, W. J. Briscoe, R. L. Workman, and I. I. Strakovsky, `http://gwdac.phys.gwu.edu/analysis/`

[11] Z. Bagdasarian et al., *First results on A_y analyzing power measurements in pp elastic scattering*, IKP Annual Report 2013, `http://collaborations.fz-juelich.de/ikp/anke/annual/Annual_Report_13.shtml`

[12] M. Haji-Said et al., Phys. Rev. C **36** (1987) 2010.

[13] D. Chiladze et al., Phys. Rev. ST-AB, **9** (2006) 050101.

[14] B. Gou et al., *Commissioning of the polarized deuterium gas target at ANKE*, IKP Annual Report 2013, `http://collaborations.fz-juelich.de/ikp/anke/annual/Annual_Report_13.shtml`